JACS

JOURNAL OF THE AMERICAN CHEMICAL SOCIETY

Article

Hydrogen Isotope Labeling of Pharmaceuticals Via Dual Hydrogen Isotope Exchange Pathways Using CdS Quantum Dot Photocatalyst

Rajendra Maity, Otto Dungan, Frédéric A. Perras, Jingwei Li,* Daohua Liu, Sumei Ren, Dan Lehnherr, Zheng Huang, Eric M. Phillips, Moses Adeyemo, Joseph Frimpong, Timothy Quainoo, Zhen-Fei Liu, and Long Luo*

Cite This: https://doi.org/10.1021/jacs.4c13857

Read Online

ACCESS | 📊 Metrics & More | 📑 Article Recommendations | 🆂�🄸 Supporting Information

- well-established dual HIE pathway
- multiple-site high D/T labeling
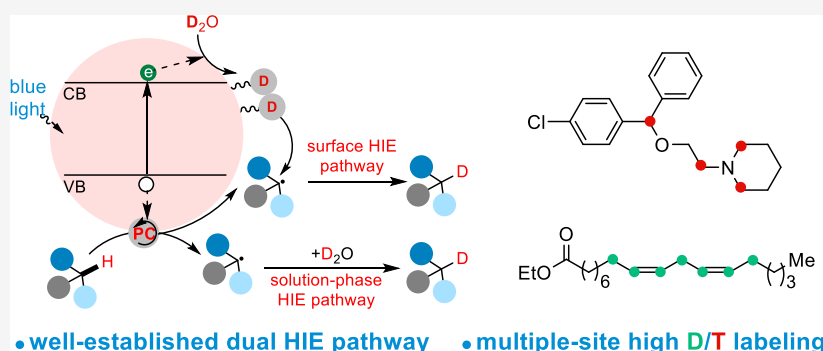
ABSTRACT: Isotopic labeling is a powerful technique extensively used in the pharmaceutical industry. By tracking isotope-labeled molecules, researchers gain unique and invaluable insights into the pharmacokinetics and pharmacodynamics of new drug candidates. Hydrogen isotope labeling is particularly important as hydrogen is ubiquitous in organic molecules in biological systems, and it can be introduced effectively through late-stage hydrogen isotope exchange (HIE). However, hydrogen isotope methods that simultaneously label multiple sites with varying types of C−H bonds in the different types of molecules are still lacking. Herein, we demonstrate a heterogeneous photocatalytic system using a CdS quantum dot catalyst that proceeds via a unique dual HIE pathway mechanism—one occurs in the reaction solution and the other on the catalytic surface—to address it. This unique mechanism unlocked several unique labeling capabilities, including simultaneous labeling of multiple and challenging sites such as secondary α-amino, α-ethereal, allyl, and vinyl sites, providing great versatility in practical uses for pharmaceutical labeling.

■ INTRODUCTION

Isotopic labeling is a powerful technique extensively used in the pharmaceutical industry.[1−4] This technique involves incorporating either stable isotopes, such as deuterium (D) and carbon-13 (^{13}C), or radioactive isotopes, such as tritium (T) and carbon-14 (^{14}C), into molecules. By tracking these labeled molecules, researchers gain unique and invaluable insights into the pharmacokinetics and pharmacodynamics of new drug candidates. Such information is critical to understanding how drugs are absorbed, distributed, metabolized, and excreted (ADME studies) in living organisms. It also provides unique tools to study the detailed mechanisms of drug action and metabolism at the molecular level without significantly altering the chemical properties of the compounds. Stable isotope-labeled (SIL) compounds are broadly used as internal standards for accurately analyzing clinical samples. The use of isotope-labeled compounds significantly accelerates drug development, reduces the time-to-market, and lowers drug development costs.

Hydrogen isotope labeling is particularly important as hydrogen is present in all organic molecules in biological systems.[5,6] Most recently, there has also been pronounced interest in developing deuterated drugs in which D incorporation may improve the pharmacokinetics, leading to enhancement of efficacy and safety.[7] Deutetrabenazine, which is used for the treatment of chorea associated with Huntington's disease, became the first deuterated drug to receive U.S. Food and Drug Administration approval in 2017.[8]

Requirements of hydrogen isotope labeling vary by their targeted applications (Figure 1a). For example, when deuterated compounds are used as an internal standard for
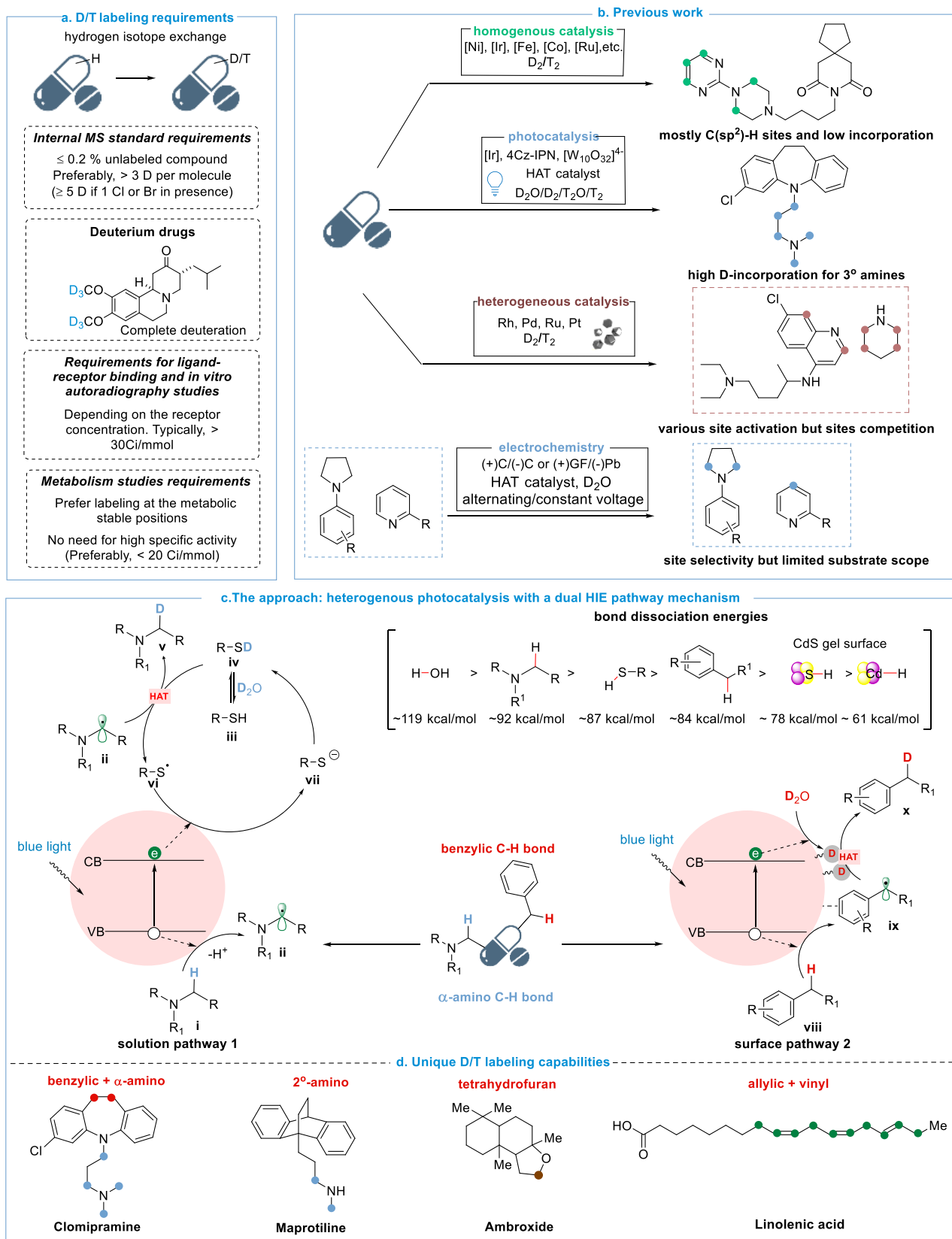
Figure 1. Background and proposed HIE method. (a) General D/T labeling requirements for various applications in the pharmaceutical industry. (b) Existing HIE methods. (c) Proposed heterogeneous photocatalytic HIE method using a CdS QD gel catalyst that proceeds via a dual HIE pathway mechanism. (d) Unique hydrogen isotope labeling capabilities of our method, including multiple site labeling, labeling α-C−H bonds of 2° amines and ethers, and allyl and vinyl sites.
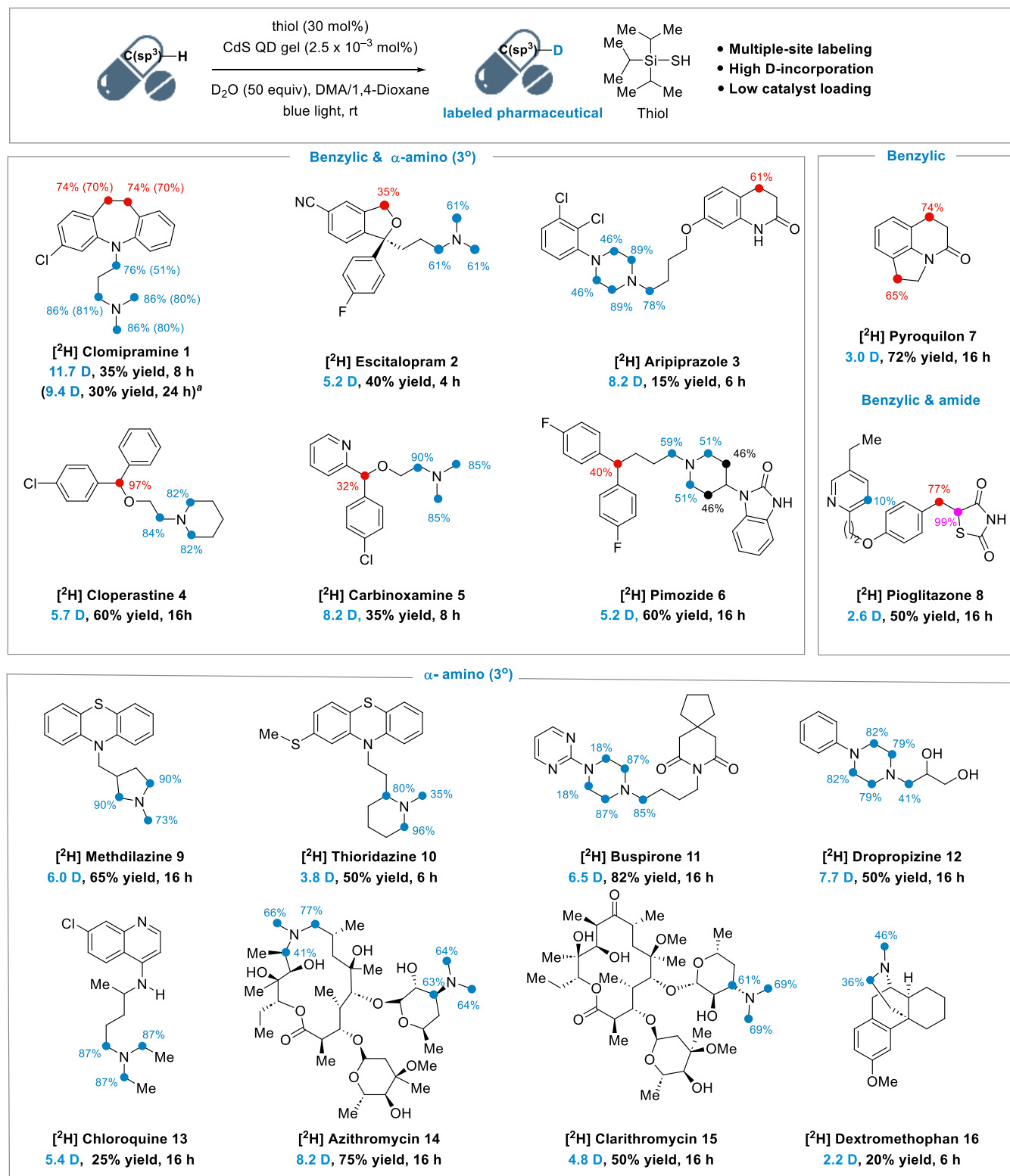
Figure 2. continued
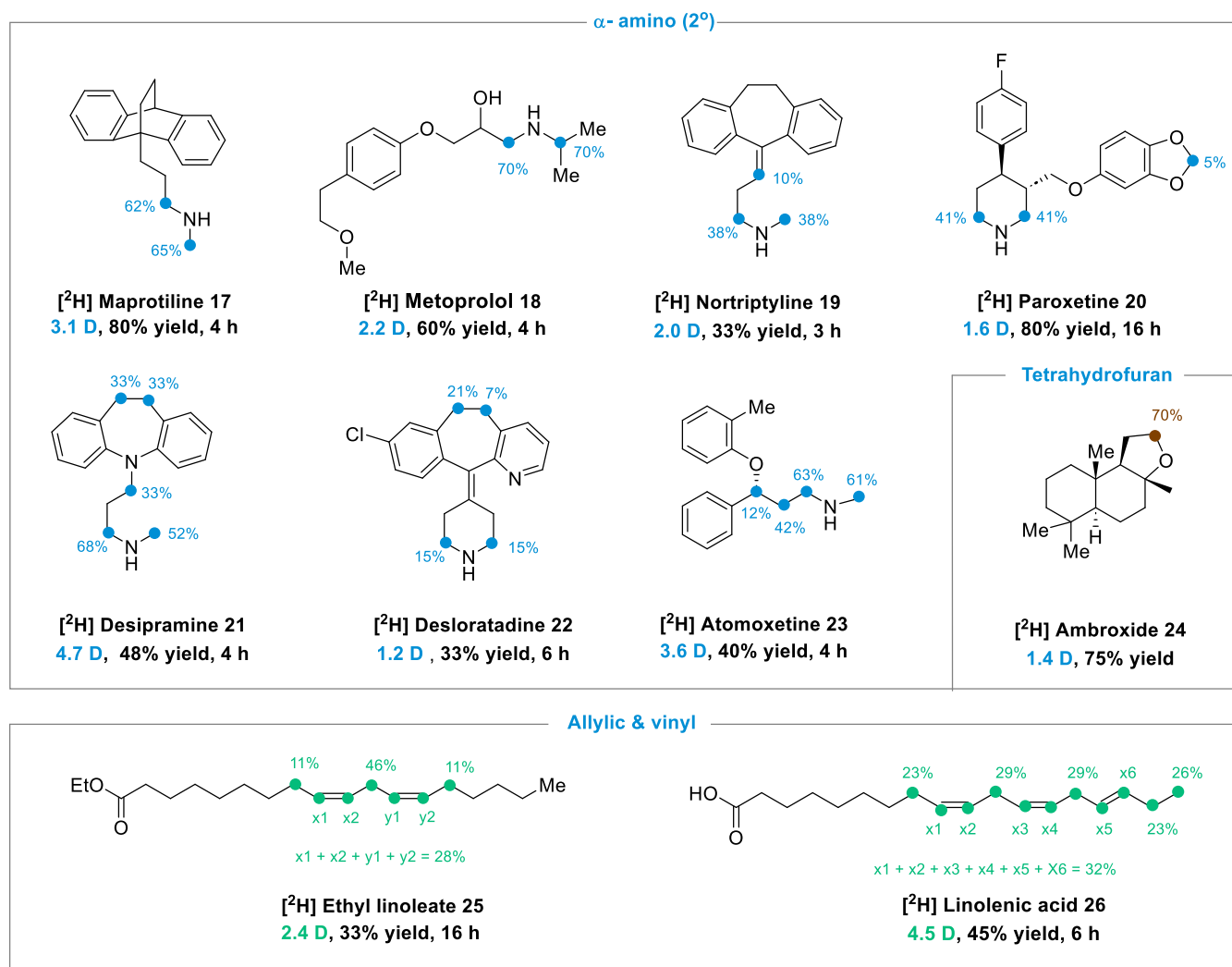
Figure 2. Scope for the H/D exchange of pharmaceuticals. Reaction conditions: substrate (0.2 mmol, 1.0 equiv), DMA or dioxane (2 mL, 0.1 M), triisopropylsilanethiol (0.06 mmol, 0.3 equiv), D_2O (10 mmol, 50 equiv) and CdS gel (125 μL, 2.5 × 10^{-3} mol %); [a]2 mmol scale reaction data for substrate **1**.

the liquid chromatography−mass spectrometry analysis of small molecules, the mass increase for the SIL should be larger than 3 Ds per molecule (≥5 D atoms if one Cl or Br atom is present) and the remaining unlabeled species in the batch should be lower than 0.2% to ensure proper resolution from the mass signals of an unlabeled analyte.[9] Low-specific activity T-labeled compounds that are labeled at a metabolically stable position are often needed for metabolism studies, such as bile duct cannulation studies in rats, to support the ADME profiling of pharmaceuticals.[10] Meanwhile, high specific activity is often required to study specific pharmacological interactions between a radiolabeled ligand and its target[11] and in autoradiography imaging.[12]

Hydrogen isotope exchange (HIE) is the most attractive approach to D/T-labeling as it allows rapid and direct isotope incorporation into pharmaceuticals at a late stage. Current HIE strategies include the following: (i) homogeneous catalysis using transition metal complexes such as [Ir],[9,10] [Co],[11] [Ni],[12] and [Fe],[13] and alkali metal amides;[14,15] (ii) photoredox catalysis using molecular photocatalysts such as [Ir], decatungstate[16] and 4Cz-IPN[17−20] coupled with a hydrogen atom transfer (HAT) catalyst such as thiol or transition metalhydride, (iii) heterogeneous catalysis using metal nano-

particles such as Ru,[21,22] Rh,[23] Ir,[10] and Pt,[24] and more recently, (iv) electrochemical methods that generate radical or ionic intermediates for D incorporation.[25−27]

Each HIE strategy's main advantages and limitations are listed in Figure 1b. First, homogeneous catalysis methods typically install D/T at specific aromatic $C(sp^2)$−H sites next to a directing group.[14,28] Next, photoredox catalysis methods mainly incorporate D/T at α-amino and formyl C−H bonds of drug molecules.[16−18,29] In comparison, heterogeneous catalysis methods using metal particles could label different types of sites. The shortcomings of current heterogeneous catalysis are (i) the use of high concentrations of radioactive tritium gas to achieve high T incorporation and (ii) when multiple sites are present in a molecule, the competition for the catalyst surface binding sites limits the overall labeling efficiency.[21,23] Electrochemical HIE methods are in their infancy and have only been demonstrated on simple amines and pyridines.[25,26] Overall, all these methods are mostly restricted to targeting one specific type of site. HIE methods that consistently and simultaneously label multiple sites with different C−H bond types are still lacking, which is important to ensure high D/T incorporation for applications as internal standards for the liquid chromatography−mass spectrometry analysis and radiolabeled tracers for

studying specific pharmacological interactions and auto-radiography imaging.

RESULTS AND DISCUSSION

Method Design and Reaction Development. Here, we designed a heterogeneous photocatalytic HIE method to address the unmet needs for multiple-site labeling of pharmaceuticals (Figure 1c). In our design, we proposed to use CdS QD gels—a 3-dimensional mesoporous network of CdS QDs with most surface ligands removed (Figures S1 and S2)[30−32]—as the photocatalyst. Metal chalcogenide quantum dots (QDs), including CdS and CdSe, are a group of emerging photocatalysts that enable unique organic transformations such as direct photocatalytic hydrogen atom abstraction,[33] radical−radical cross-coupling,[34] and regioselective [2 + 2] cyclic addition.[35,36] We hypothesized that this CdS photocatalytic system could provide two parallel HIE pathways for simultaneously labeling different sites: one in solution and the other on the catalyst surface. In solution, the CdS catalyst would generate radical intermediates via single electron transfer events upon photoexcitation. The formed radicals would then react with a solution-phase HAT catalyst, such as a deuterated thiol, to be deuterated. In parallel, the CdS catalyst surface would stabilize radical intermediates and D atoms, mediating the transfer of D atoms to the surface-bound intermediates.

The solution pathway behaves similarly to photoredox catalysis methods using molecular photocatalysts.[18] Because the S−H bond dissociation energy (BDE) of thiols (≈87.0 kcal/mol) is relatively large, thiols cannot efficiently transfer D/T atoms to C−H bonds with low BDEs such as benzylic C−H bonds (≈74 to 88 kcal/mol).[37] This limitation can be overcome via the surface pathway using the H atoms adsorbed on the CdS surface with calculated BDEs of ≈78.0 kcal/mol at the S site and ≈61.0 kcal/mol at the Cd site (Figure S4). The two independent pathways enable the simultaneous labeling of pharmaceuticals at different types of sites, such as benzylic and α-amino sites, while minimizing the competition for catalytic surface sites (Figure 1d). In addition, Cd chalcogenide surfaces are known to stabilize secondary (2°) amines,[38] activate cyclic ethers,[33] and stabilize allylic and vinylic radicals,[18,34,39] facilitating their HIE reactions.

We initiated our studies using a commercial antidepressant, clomipramine (1), which contains both an alkyl amine moiety and benzylic sites, as a model substrate. We used triisopropylsilanethiol as the solution-phase HAT catalyst and D$_2$O as a D source (Figure 2). The results show that the CdS QD gel photocatalyst with the loading of merely 2.5×10^{-3} mol % (Figure S3) delivered the deuterated product [^{2}H]1 with an impressive 11.7 D/molecule with less than <0.1% of the unlabeled compound remaining (Figure S9). The two benzylic and four α-amino sites were highly deuterated to levels of 76% and 74−86%, respectively (Figure 2). In comparison, existing photoredox protocols using molecular photocatalysts primarily activate the α-amino C−H bonds and occasionally benzylic C−H bonds with low D incorporation, giving a total of 6 or 7 D/molecule (Figure S11).[18] The yield was slightly lower than that using the photoredox protocols due to the possible additional decomposition pathways initiated at the benzylic sites. Despite varying the solvent, thiol type, light intensity, reaction time, D$_2$O equivalent, and base addition, effective D incorporation at both sites remained unchanged (Tables S1−S6). Comparable results were obtained

with a scale-up reaction (Figure S12). The recovered CdS photocatalyst showed similar reactivity after three runs, and no noticeable morphology changes were observed after the recycling experiments (Figure S13). The analysis of residual Cd in the purified [^{2}H]1 shows only ∼2.3 part-per-million Cd, suggesting no significant metal leaching (see Supporting Information). The light on/off experiment showed that D-labeling increased only when the light was on, indicating that the HIE reaction is a light-driven process (Figure S14). A radical capture experiment using methyl vinyl ketone as the radical acceptor showed the formation of mono/dialkylated products of 1, suggesting that the radical centers are generated under HIE reaction conditions, possibly at various sites of 1. Unfortunately, the attempt to isolate the alkylated products was unsuccessful due to the complexity of the reaction mixture.

Substrate Scope. The optimal protocol was applied to 26 commercially available drugs. We first tested drug molecules consisting of benzylic and tertiary (3°) alkyl amine scaffolds (2−6). Efficient D incorporation at both types of sites for these substrates was obtained, similar to 1 (Figure 2). For example, aripiprazole (3) accomplished 61% deuteration at its benzylic position in a lactam ring (3-fold higher than the existing method, Figure S11) and 46%−89% deuteration at its piperazine α-amino sites. High labeling efficiency was also achieved at acyclic benzylic positions of cloperastine (4, 97%), carbinoxamine (5, 32%), and pimozide (6, 40%) while achieving high labeling efficiencies of 50% to 90% at their α-amino positions. In certain cases, β-amino positions were also deuterated with moderate efficiencies (e.g., 46% for 6), possibly through an iminium intermediate.[18]

Without alkyl amine moieties, the HIE at benzylic positions remained efficient, with a D incorporation of 65% and 74% for pyroquilon (7) and 77% for pioglitazone (8). The α-position adjacent to the carbonyl carbon of 8 also completely exchanged with D. Drug molecules with only tertiary alkyl amine scaffolds also showed high D-incorporation at their α-amino sites, producing [^{2}H]9-methdilazine (6.0 D/molecule), [^{2}H]10-thioridazine (3.8 D/molecule), [^{2}H]11-buspirone (6.5 D/molecule), [^{2}H]12-dropropizine (7.7 D/molecule) and [^{2}H]13-chloroquine (5.4 D/molecule). Macrocyclic drugs, such as [^{2}H]14-azithromycin and [^{2}H]15-clarithromycin, delivered D-incorporation values of 8.2 and 4.8 D, respectively. In the case of dextromethorphan (16), only its α-amino positions were deuterated, possibly because its T-shaped configuration caused steric hindrance for the interaction between the benzylic C−H bond and the CdS surface.

Next, we expanded the substrate scope to drugs with secondary amine and benzylic scaffolds. Directly labeling secondary amines is challenging because homogeneous metal catalysts often coordinate with them, preventing the delivery of HIE products.[40,41] There are limited reported HIE methods for 2° amine deuteration with scattered examples.[23,42,43] Our method smoothly labeled the α-position of 2° amines with a D incorporation of 40% to 70% and a good yield of 30% to 80% at room temperature ([^{2}H]17 to [^{2}H]23). Benzylic site labeling was, however, suppressed for these substrates, possibly because the 2° amine sites outcompeted benzylic sites for CdS surface sites, blocking the surface pathway for benzylic site labeling. During the HIE reactions, a wide range of functional groups such as alcohol, halogen (F and Cl), cyano, allyl, amide, carbonyl, pyridine, and thio/ether groups were well tolerated, and the stereogenic centers were retained (Figures S16−S18).
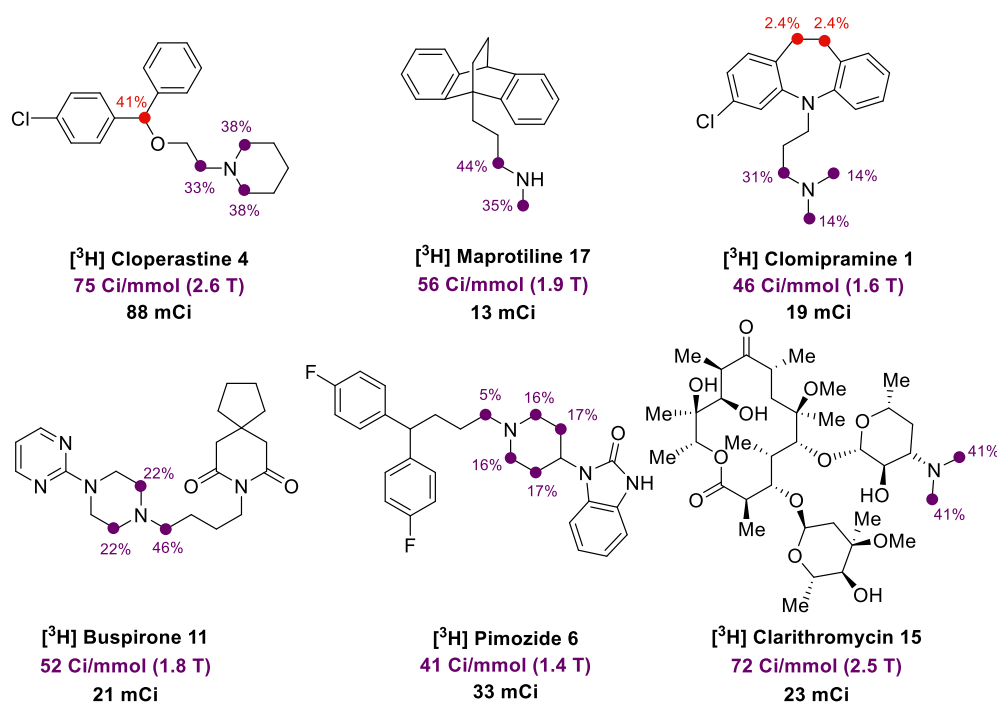
Figure 3. Scope for the H/T exchange of pharmaceuticals. Reaction conditions: substrate (1 μmol), CdS gel photocatalyst (10 μL, 40 × 10^{-3} mol %), thiol catalyst (triisopropylsilanethiol, 30 mol %). T$_2$O (generated from 2 Ci of T$_2$ and PtO$_2$). The reaction was irradiated in the integrated photoreactor at 65% intensity.

Labeling the α-C−H bonds of cyclic ethers, such as ambroxide (24, 1.4 D/molecule), and allylic and vinyl C−H bonds of poly alkenes, such as ethyl linoleate (25, 2.4 D/molecule) and linolenic acid (26, 4.5 D/molecule) were also successful. Poly alkene deuteration is difficult because of possible double bond migration and hydrogenation under the HIE conditions. The H/D exchange results above clearly demonstrated the versatility of our heterogeneous photocatalytic HIE method for labeling various C−H bonds.

Based on the optimized deuterium HIE conditions, further optimization was performed for tritiation (Tables S9−S13). The tritiation was conducted at a 1 μmol scale with a reduced equivalency of T$_2$O. High-specific activity T$_2$O was generated via a reaction of PtO$_2$ and T$_2$ gas in dioxane under modified conditions (Figure S19).[44] We were delighted that successful tritiations were achieved after slightly tuning the reaction parameters, such as increasing the QD loading, reducing the photo intensity, and/or shortening the reaction time (Figure 3). Cloperastine (4) was successfully labeled under 2 h irradiation to give 88 mCi of product at 75 Ci/mmol, resulting in doubled T incorporation compared with the reported method (Figure S11).[18] Not surprisingly, T labeling was achieved on both benzylic (41%) and α-amine C(sp^3)−H sites (33% and 38%), consistent with the deuteration results. Other substrates were also efficiently labeled with this method, including dibenzazepine clomipramine (1, 46 Ci/mmol, 45 min), piperidine pimozide (6, 41 Ci/mmol, 2 h), piperazine buspirone (11, 52 Ci/mmol, 2 h), and macrolide clarithromycin (15, 72 Ci/mmol, 4 h). For 1 and 6, the limited T incorporation at the benzylic site could be attributed to the reduced reaction time in tritiation to prevent decomposition. Despite the significant advancements in HIE method development in recent years, certain functional groups, such as secondary amines, are still not amenable to generating high-specific activity T tracers. Limited reports in the literature

showed that HIE using Ru-based catalysts only produced low specific activity, even with excessive amounts of T$_2$O of up to 20 Ci.[45−47] With this QD-catalyzed HIE method, we successfully labeled a secondary amine, 17, at the α-position with high specific activity (56 Ci/mmol). This approach opened up the possibility of direct tritium labeling of secondary amines.

Overall, the T-labeled drugs generated through our methodology exhibited high specific activity with >40 Ci/mmol while achieving diverse labeling positions with expanded substrate scope. They hold great potential for general drug metabolism and pharmacokinetic studies and meet the requirements for low-density receptor binding studies, where high specific activity is crucial for accurate measurements.

Mechanistic Studies. We performed a series of mechanistic experiments to gain comprehensive insights into the HIE mechanism. First, we confirmed that the HIE reactions at the benzylic and 3° α-amino C−H sites occurred simultaneously, rather than sequentially, by monitoring the D incorporation evolution at each site of 1 (Figure 4a). However, the HIE reaction rate did vary by site: the highest at the C5 position, followed by the C6 and C7, and last C1, C2, and C3 (Table S5).

Next, we identified that the HIE at the benzylic and 3° α-amino C−H sites proceeded via two independent pathways. As illustrated in Figure 4b, our proposed HIE reaction undergoes a dual HIE pathway mechanism, in which thiol is the HAT catalyst for the solution pathway, and CdS surface is the HAT catalyst for the surface pathway. Without thiol, the solution pathway would be shut down, whereas the surface pathway would not. Figure 4c compares the HIE results for 1 with and without thiol. We found that removing thiol inhibited the HIE at its α-amino sites with D incorporation of 2 to 8%, whereas its benzylic C−H sites still showed moderate D incorporation of ~38%. With the thiol loading gradually increased from 0 to
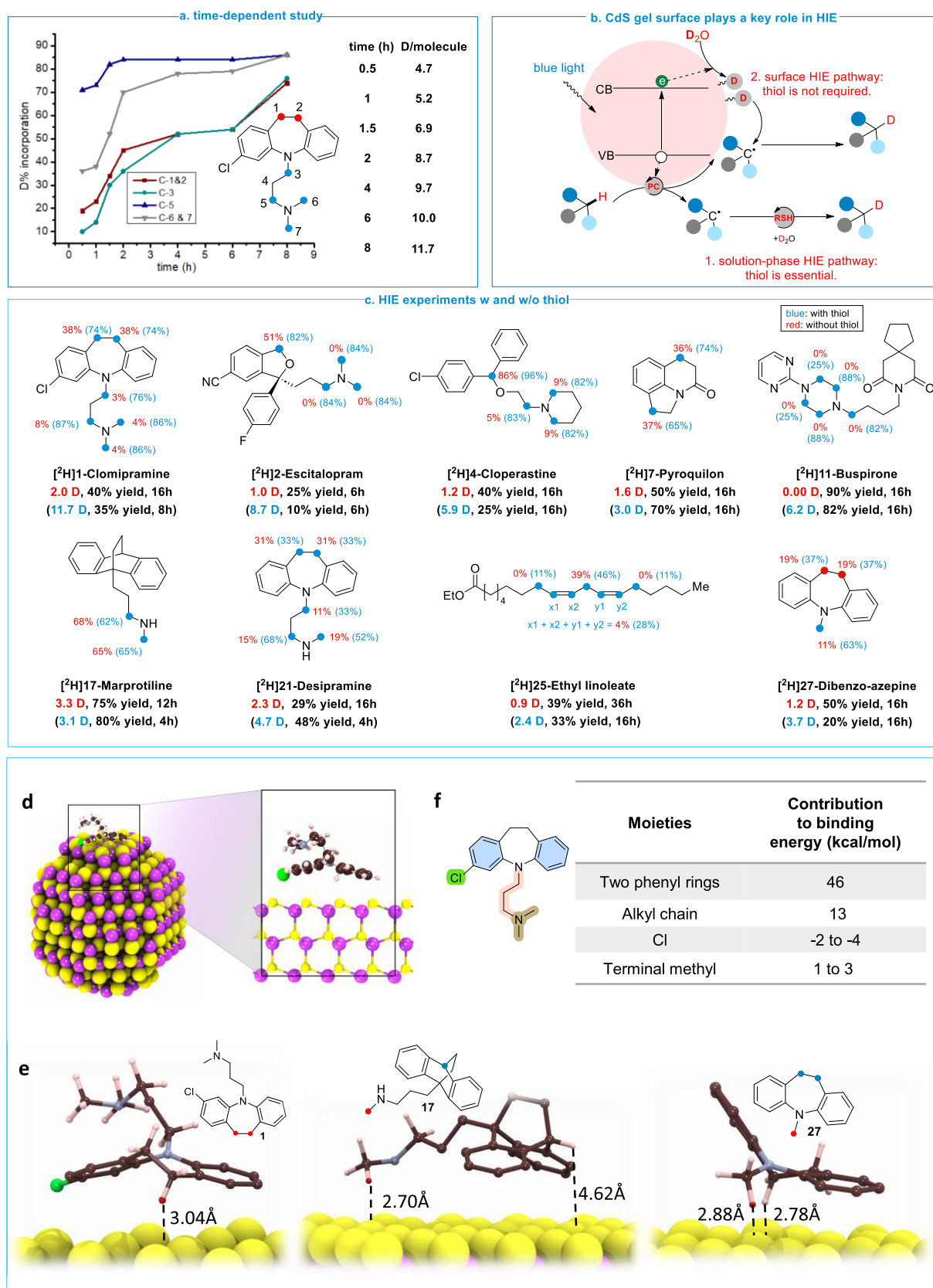
Figure 4. Mechanistic studies. (a) % D incorporation at different sites as a function of reaction time. (b) Proposed dual HIE pathway mechanism. (c) HIE experiment results with and without thiol catalyst. Reaction conditions: substrate (0.2 mmol, 1.0 equiv), DMA or dioxane (2 mL, 0.1 M), D_2O (10 mmol, 50 equiv) and CdS gel (125 μL, 2.5×10^{-3} mol %). (d) Size comparison between a CdS QD and **1**. (e) Binding energy contribution of different moieties of **1**. (f) Stable binding conformation of **1**, **17**, and **27** on a CdS surface.
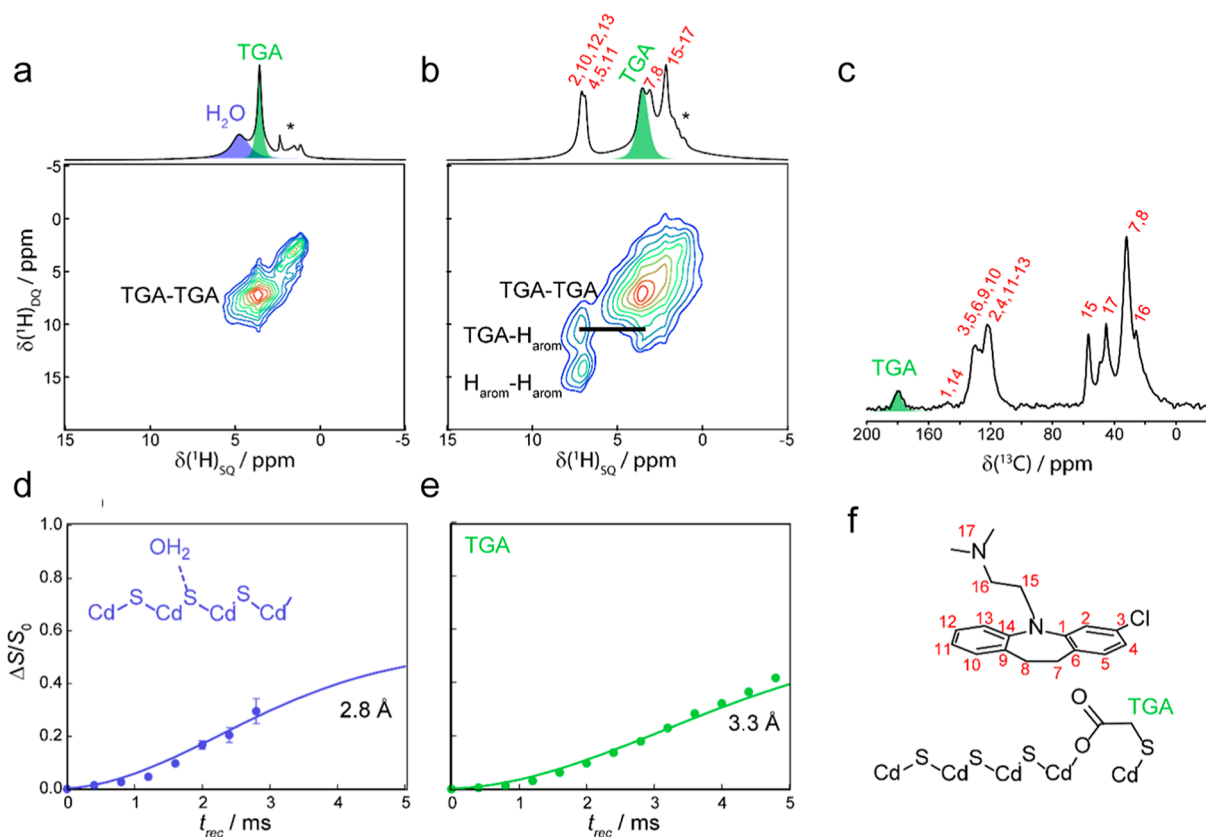
Figure 5. Solid-state NMR studies. ^{1}H 1D fast-MAS and 2D DQ/SQ correlation spectra acquired for (a) bare CdS gel and (b) one washed with a CH_2Cl_2 solution of **1**. (c) ^{13}C CPMAS NMR spectrum of the latter material. ^{1}H$-^{111}$Cd DE-S-REDOR dephasing curves and fits for the signals resonating at (d) 4.7 ppm and (e) 3.6 ppm assigned to physiosorbed water and thioglycolate, respectively. (f) A model of surface adsorption of **1** agrees with the observed correlations between ^{1}H$-^1$H and ^{1}H$-^{111}$Cd.

30 mol %, the D incorporation gradually increased to 74% for the benzylic C−H bonds, whereas it soared from 4% to 86% for α-amino C−H bonds (Table S7). Similar D labeling differences between with and without thiol were observed for other drugs with both benzylic and tertiary amine scaffolds, such as **2** and **4** (Figure 4c). When only benzylic sites are present, like in **7**, its D incorporation was successful without thiol. In contrast, the absence of thiol failed to incorporate any deuterons into **11**, which has only 3° α-amino sites. These findings indicate that the HIE at 3° α-amino sites almost exclusively proceeded via the solution pathway that required thiol as the HAT catalyst, whereas the HIE at the benzylic site primarily proceeded via the surface pathway.

We further used trioctylphosphine oxide ligand-capped CdS QDs as a negative control to block the surface pathway. We observed that the D incorporation at benzylic sites of **1** was low (only 11%), whereas its α-amino sites were less affected (29% to 83%) under the optimal HIE conditions (Table S8). Without thiol, both types of sites became silent (Table S7). This observation further supports our assignments on the two HIE pathways. In addition, we also tested commercially available CdS powder. We observed a similar D labeling pattern as QD gels with and without thiol (Tables S7 and S8), indicating the unique HIE reactivity is inherent to different CdS materials.

During the substrate scope development, we found that the presence of secondary amine moieties suppressed the benzylic site labeling. We attributed it to 2° amines outcompeting benzylic sites over the CdS surface sites. To test this

hypothesis, we carried out the HIE reaction without thiol for **17** and **21**. Interestingly, the absence of thiol did not turn off the D incorporation at 2° α-amino positions (Figure 4c), supporting the proposed explanation. For example, [^{2}H]**17** showed almost identical D incorporation with and without thiols (3.1 vs 3.3 D/molecule), suggesting that the HIE at its secondary α-amino sites exclusively proceeded via the surface pathway. In the case of conjugated poly alkenes such as **25**, only the allyl site between the alkenes was labeled in the absence of thiol. This result suggests that these substrates interact with the CdS surface via their alkene moiety during the HIE reaction.

As alluded to above, the D labeling through the surface pathway is determined by how a drug molecule interacts with the CdS catalyst surface. The stronger surface interaction a moiety has, the more likely its C−H bonds are labeled via the surface pathway. To decipher the above D-labeling results, we computed the binding conformations of drug molecules on a CdS QD surface. Figure 4d shows the size comparison between **1** and one CdS QD in the gel catalyst. We varied the molecular orientation on the CdS surface and calculated the binding energies of different conformations (Figure S5). Figure 4f shows one stable binding confirmation of **1** on the CdS surface. From the results of different conformations, we deduced each moiety's contribution in **1** to the total binding energy (Figure S5). Figure 4e shows the two phenyl rings are the strongest binding moieties with a predominantly dispersive binding energy contribution of 46 kcal/mol, three times stronger than the alkyl amine chain (13 kcal/mol). This

344 suggests that **1** preferentially binds to the CdS surface through
345 the phenyl rings.

346   Similar simulations were conducted for **17**. In its strongest
347 binding conformation, the amine moiety is bound to the CdS
348 surface (Figures 4f and S8). However, due to its bicyclic
349 structure, the distance between the benzylic C−H and CdS
350 surface is ~4.62 Å, which is prohibitive for the HAT process
351 (typically, the HAT distance should be ≤3 Å according to the
352 Landau−Zener model).[48] This finding is consistent with the
353 experimental result that no D-labeling was observed at benzylic
354 sites of **17** (Figure 4c). In addition, we studied dibenzo-
355 azepine (**27**), which has a similar structure as **1** but replaces
356 the alkyl amine chain of **1** with a methyl group. The C−H
357 bonds on the methyl group of **27** are free to rotate. They thus
358 could have a similar distance of ~2.8 Å to the CdS surface as
359 benzylic C−H bonds (Figure 4f). We observed comparable D-
360 labeling at both sites (11% vs 19%) in the absence of thiol
361 (Figure 4c). These results indicate that the distance between
362 the H atom to be exchanged and the CdS catalytic surface
363 dictates the D labeling efficiency via the surface pathway.

364   Lastly, we employed an array of through-space dipolar-based
365 solid-state nuclear magnetic resonance (NMR) methods to
366 experimentally validate the theoretically predicted binding
367 conformation of **1** on the CdS surface. The ^{1}H fast-magic-angle
368 spinning (FMAS) NMR spectra acquired for bare CdS QD gel
369 and one that was exposed to a solution of **1** are shown in
370 Figure 5a,b. We observed in the bare gel ^{1}H NMR signals
371 belonging to a trace amount of trioctylphosphine oxide ligands
372 used in the QD synthesis (marked by an asterisk) and signals
373 resonating at 3.6 and 4.7 ppm. The signal at 3.6 ppm originates
374 from the methylene group of residual thioglycolate ligands
375 from the gel synthesis, while the signal at 4.7 ppm is assigned
376 to physisorbed water or potentially surface S−H groups. Once
377 **1** was added, the signal at 4.7 ppm was removed and replaced
378 by a variety of signals belonging to the adsorbed **1** (Figure 5b,
379 assignments in Figure 5f). The adsorbed **1** was also apparent
380 from a ^{13}C Cross-Polarization Magic-Angle-Spinning
381 (CPMAS) NMR spectrum (Figure 5c) that also displayed a
382 slightly shifted resonance from the thioglycolate carboxyl,
383 suggesting Cd coordination. We performed ^{1}H−^{111}Cd double-
384 echo symmetry-based rotational-echo double-resonance (DE-
385 S-REDOR) experiments to probe the interaction between
386 these species and the CdS surface (Figure 5d,e).[49,50] We only
387 observed dipolar dephasing from the resonances at 4.7 and 3.6
388 ppm belonging to water and thioglycolate. Using previously
389 described models,[51] we fitted these data to a multispin model
390 of the CdS surface and found that the water signal is tightly
391 bound to the surface, at only 2.8 Å from the Cd layer.[49]
392 Similarly, the thioglycolate CH$_2$ was closer to the surface than
393 would be expected from bidentate coordination at 3.3 Å from
394 the Cd layer, suggesting the secondary coordination of the
395 thiol. This is also consistent with our lack of detection of a
396 thiol ^{1}H NMR signal.

397   We additionally performed ^{1}H homonuclear double-
398 quantum correlation experiments (DQ/SQ, Figure 5a,b,
399 bottom) to probe ^{1}H−^{1}H proximities, which are more sensitive
400 to long-range interactions than ^{1}H−^{111}Cd interactions due to
401 both the larger gyromagnetic ratio of ^{1}H and its 100% natural
402 abundance (as opposed to 12.8% for ^{111}Cd).[52,53] While we
403 could not detect **1**−^{111}Cd interactions, we did see a strong
404 correlation at a double-quantum chemical shift of 10.8 ppm
405 from a proximity between the aromatic ^{1}H's of **1** and the
406 surface-bound thioglycolate (highlighted by the horizontal line

in Figure 5b). The only logical explanation for this correlation, 407
and the DE-S-REDOR results, is that the CdS surface was 408
partially terminated by thioglycolate ligands, and **1** exists at the 409
surface near these sites. The starkly stronger correlation 410
between these aromatic ^{1}H's and the surface sites, as compared 411
to the alkyl ^{1}H's, nevertheless shows that **1** prefers to adsorb 412
on the surface through its ring structure, in agreement with the 413
theoretical model in Figure 4d and the preferred deuteration 414
observed experimentally in Figure 4c. 415

■ CONCLUSION 416

In summary, we developed a new heterogeneous photocatalytic 417
hydrogen isotope labeling method for pharmaceuticals. 418
Mechanistic studies revealed a dual HIE pathway mechanism. 419
This unique mechanism unlocked several unique labeling 420
capabilities, including simultaneous labeling of multiple and 421
challenging sites such as 2° α-amino, α-ethereal, allyl, and vinyl 422
sites, providing great versatility in practical uses for 423
pharmaceutical labeling. 424

■ ASSOCIATED CONTENT 425

■ AUTHOR INFORMATION 434

Corresponding Authors 435

   Jingwei Li − *Process Research and Development, Merck & Co.,* 436
   Inc., Rahway, New Jersey 07065, United States; 437
   Email: jingwei.li1@merck.com 438

   Long Luo − *Department of Chemistry, University of Utah, Salt* 439
   Lake City, Utah 84112, United States; Department of 440
   Chemistry, Wayne State University, Detroit, Michigan 48202, 441
   United States; orcid.org/0000-0001-5771-6892; 442
   Email: long.luo@utah.edu 443

Authors 444

   Rajendra Maity − *Department of Chemistry, University of* 445
   Utah, Salt Lake City, Utah 84112, United States 446

   Otto Dungan − *Process Research and Development, Merck &* 447
   Co., Inc., Rahway, New Jersey 07065, United States; 448
   orcid.org/0009-0007-9426-4611 449

   Frédéric A. Perras − *Chemical and Biological Sciences* 450
   Division, Ames National Laboratory, Ames, Iowa 50011, 451
   United States; Department of Chemistry, Iowa State 452
   University, Ames, Iowa 50011, United States 453

   Daohua Liu − *Department of Chemistry, Wayne State* 454
   University, Detroit, Michigan 48202, United States 455

   Sumei Ren − *Process Research and Development, Merck &* 456
   Co., Inc., Rahway, New Jersey 07065, United States; 457
   orcid.org/0000-0002-5163-0489 458

   Dan Lehnherr − *Process Research and Development, Merck &* 459
   Co., Inc., Rahway, New Jersey 07065, United States; 460
   orcid.org/0000-0001-8392-1208 461

   Zheng Huang − *Process Research and Development, Merck &* 462
   Co., Inc., Rahway, New Jersey 07065, United States; Present 463
   Address: Analytical Chemistry Development and Supply, 464

Merck & Co., Inc., Rahway, New Jersey 07065, United States; ● orcid.org/0000-0003-0876-5369

Eric M. Phillips − *Process Research and Development, Merck & Co., Inc., Rahway, New Jersey 07065, United States;* ● orcid.org/0000-0003-3530-8876

Moses Adeyemo − *Department of Chemistry, Wayne State University, Detroit, Michigan 48202, United States;* ● orcid.org/0000-0002-0493-3145

Joseph Frimpong − *Department of Chemistry, Wayne State University, Detroit, Michigan 48202, United States*

Timothy Quainoo − *Department of Chemistry, Wayne State University, Detroit, Michigan 48202, United States*

Zhen-Fei Liu − *Department of Chemistry, Wayne State University, Detroit, Michigan 48202, United States;* ● orcid.org/0000-0002-2423-8430

Complete contact information is available at:
https://pubs.acs.org/10.1021/jacs.4c13857

Notes

The authors declare no competing financial interest.

■ ACKNOWLEDGMENTS

■ REFERENCES

(1) Elmore, C. S. The use of isotopically labeled compounds in drug discovery. *Annu. Rep. Med. Chem.* **2009**, *44*, 515−534.

(2) Elmore, C. S.; Bragg, R. A. Isotope chemistry; a useful tool in the drug discovery arsenal. *Bioorg. Med. Chem. Lett.* **2015**, *25* (2), 167−171.

(3) Christian, J. E. Radioisotopes in the Pharmaceutical Sciences and Industry. *J. Pharm. Sci.* **1961**, *50* (1), 1−13.

(4) Mutlib, A. E. Application of Stable Isotope-Labeled Compounds in Metabolism and in Metabolism-Mediated Toxicity Studies. *Chem. Res. Toxicol.* **2008**, *21* (9), 1672−1689.

(5) Kopf, S.; Bourriquen, F.; Li, W.; Neumann, H.; Junge, K.; Beller, M. Recent Developments for the Deuterium and Tritium Labeling of Organic Molecules. *Chem. Rev.* **2022**, *122* (6), 6634−6718.

(6) Gant, T. G. Using deuterium in drug discovery: leaving the label in the drug. *J. Med. Chem.* **2014**, *57* (9), 3595−3611.

(7) Di Martino, R. M. C.; Maxwell, B. D.; Pirali, T. Deuterium in drug discovery: progress, opportunities and challenges. *Nat. Rev. Drug Discovery* **2023**, *22* (7), 562−584.

(8) Gupta, H.; Perkins, W.; Stark, C.; Kikkeri, S.; Kakazu, J.; Kaye, A.; Kaye, A. D. Deutetrabenazine for the treatment of chorea associated with Huntington's disease. *Health Psychol. Res.* **2022**, *10* (5), 36040.

(9) Kerr, W. J.; Knox, G. J.; Paterson, L. C. Recent advances in iridium(I) catalysis towards directed hydrogen isotope exchange. *J. Labelled Compd. Radiopharm.* **2020**, *63* (6), 281−295.

(10) Daniel-Bertrand, M.; Garcia-Argote, S.; Palazzolo, A.; Mustieles Marin, I.; Fazzini, P. F.; Tricard, S.; Chaudret, B.; Derdau, V.; Feuillastre, S.; Pieters, G. Multiple Site Hydrogen Isotope Labelling of Pharmaceuticals. *Angew. Chem., Int. Ed.* **2020**, *59* (47), 21114−21120.

(11) Palmer, W. N.; Chirik, P. J. Cobalt-Catalyzed Stereoretentive Hydrogen Isotope Exchange of C(sp^3)−H Bonds. *ACS Catal.* **2017**, *7* (9), 5674−5678.

(12) Yang, H.; Zarate, C.; Palmer, W. N.; Rivera, N.; Hesk, D.; Chirik, P. J. Site-Selective Nickel-Catalyzed Hydrogen Isotope Exchange in N-Heterocycles and Its Application to the Tritiation of Pharmaceuticals. *ACS Catal.* **2018**, *8* (11), 10210−10218.

(13) Pony Yu, R.; Hesk, D.; Rivera, N.; Pelczer, I.; Chirik, P. J. Iron-catalysed tritiation of pharmaceuticals. *Nature* **2016**, *529* (7585), 195−199.

(14) Du, H.-Z.; Li, J.; Christodoulou, S.; Li, S.-Y.; Cui, Y.-S.; Wu, J.; Ren, S.; Maron, L.; Shi, Z.-J.; Guan, B.-T. Directed Aromatic Deuteration and Tritiation of Pharmaceuticals by Heavy Alkali Metal Amide Catalysts. *ACS Catal.* **2024**, *14* (13), 9640−9647.

(15) Du, H.-Z.; Fan, J.-Z.; Wang, Z.-Z.; Strotman, N. A.; Yang, H.; Guan, B.-T. Cesium Amide-Catalyzed Selective Deuteration of Benzylic C-H Bonds with D$_2$ and Application for Tritiation of Pharmaceuticals. *Angew. Chem., Int. Ed.* **2023**, *62* (8), No. e202214461.

(16) Dong, J.; Wang, X.; Wang, Z.; Song, H.; Liu, Y.; Wang, Q. Formyl-selective deuteration of aldehydes with D$_2$O via synergistic organic and photoredox catalysis. *Chem. Sci.* **2020**, *11* (4), 1026−1031.

(17) Yang, H.; Huang, Z.; Lehnherr, D.; Lam, Y. H.; Ren, S.; Strotman, N. A. Efficient Aliphatic Hydrogen-Isotope Exchange with Tritium Gas through the Merger of Photoredox and Hydrogenation Catalysts. *J. Am. Chem. Soc.* **2022**, *144* (11), 5010−5022.

(18) Loh, Y. Y.; Nagao, K.; Hoover, A. J.; Hesk, D.; Rivera, N. R.; Colletti, S. L.; Davies, I. W.; MacMillan, D. W. C. Photoredox-catalyzed deuteration and tritiation of pharmaceutical compounds. *Science* **2017**, *358* (6367), 1182−1187.

(19) Kuang, Y.; Cao, H.; Tang, H.; Chew, J.; Chen, W.; Shi, X.; Wu, J. Visible light driven deuteration of formyl C−H and hydridic C(sp^3)−H bonds in feedstock chemicals and pharmaceutical molecules. *Chem. Sci.* **2020**, *11* (33), 8912−8918.

(20) Zhou, R.; Li, J.; Cheo, H. W.; Chua, R.; Zhan, G.; Hou, Z.; Wu, J. Visible-light-mediated deuteration of silanes with deuterium oxide. *Chem. Sci.* **2019**, *10* (31), 7340−7344.

(21) Pieters, G.; Taglang, C.; Bonnefille, E.; Gutmann, T.; Puente, C.; Berthet, J.-C.; Dugave, C.; Chaudret, B.; Rousseau, B. Regioselective and Stereospecific Deuteration of Bioactive Aza Compounds by the Use of Ruthenium Nanoparticles. *Angew. Chem., Int. Ed.* **2014**, *53* (1), 230−234.

(22) Taglang, C.; Martínez-Prieto, L. M.; del Rosal, I.; Maron, L.; Poteau, R.; Philippot, K.; Chaudret, B.; Perato, S.; Sam Lone, A.; Puente, C.; et al. Enantiospecific C-H activation using ruthenium nanocatalysts. *Angew. Chem., Int. Ed.* **2015**, *54*, 10474−10477.

(23) Levernier, E.; Tatoueix, K.; Garcia-Argote, S.; Pfeifer, V.; Kiesling, R.; Gravel, E.; Feuillastre, S.; Pieters, G. Easy-to-Implement Hydrogen Isotope Exchange for the Labeling of N-Heterocycles, Alkylamines, Benzylic Scaffolds, and Pharmaceuticals. *JACS Au* **2022**, *2* (4), 801−808.

(24) Sajiki, H.; Ito, N.; Esaki, H.; Maesawa, T.; Maegawa, T.; Hirota, K. Aromatic ring favorable and efficient H−D exchange reaction catalyzed by Pt/C. *Tetrahedron Lett.* **2005**, *46* (41), 6995−6998.

(25) Behera, N.; Gunasekera, D.; Mahajan, J.; Frimpong, J.; Liu, Z.-F.; Luo, L. Electrochemical Hydrogen Isotope Exchange of Amines Controlled by Alternating Current Frequency. *Faraday Discuss.* **2023**, *247*, 45−58.

(26) Zhao, Z.; Zhang, R.; Liu, Y.; Zhu, Z.; Wang, Q.; Qiu, Y. Electrochemical C−H deuteration of pyridine derivatives with D2O. *Nat. Commun.* **2024**, *15* (1), 3832.

(27) Shi, L.; Liu, M.; Zheng, L.; Gao, Q.; Wang, M.; Wang, X.; Xiang, J. Electrochemical γ-Selective Deuteration of Pyridines. *Org. Lett.* **2024**, *26* (20), 4318−4322.

(28) Prakash, G.; Paul, N.; Oliver, G. A.; Werz, D. B.; Maiti, D. C−H deuteration of organic compounds and potential drug candidates. *Chem. Soc. Rev.* **2022**, *51* (8), 3123−3163.

(29) Kramp, H.; Weck, R.; Sandvoss, M.; Sib, A.; Mencia, G.; Fazzini, P.-F.; Chaudret, B.; Derdau, V. In situ Generated Iridium Nanoparticles as Hydride Donors in Photoredox-Catalyzed Hydrogen Isotope Exchange Reactions with Deuterium and Tritium Gas. *Angew. Chem., Int. Ed.* **2023**, *62* (36), No. e202308983.

(30) Hewa-Rahinduwage, C. C.; Geng, X.; Silva, K. L.; Niu, X.; Zhang, L.; Brock, S. L.; Luo, L. Reversible Electrochemical Gelation of Metal Chalcogenide Quantum Dots. *J. Am. Chem. Soc.* **2020**, *142* (28), 12207−12215.

(31) Geng, X.; Liu, D.; Hewa-Rahinduwage, C. C.; Brock, S. L.; Luo, L. Electrochemical Gelation of Metal Chalcogenide Quantum Dots: Applications in Gas Sensing and Photocatalysis. *Acc. Chem. Res.* **2023**, *56* (9), 1087−1096.

(32) Mohanan, J. L.; Arachchige, I. U.; Brock, S. L. Porous semiconductor chalcogenide aerogels. *Science* **2005**, *307* (5708), 397−400.

(33) Liu, D.; Hazra, A.; Liu, X.; Maity, R.; Tan, T.; Luo, L. CdS Quantum Dot Gels as a Direct Hydrogen Atom Transfer Photo-catalyst for C−H Activation. *Angew. Chem., Int. Ed.* **2024**, *63*, No. e202403186.

(34) Huang, C.; Qiao, J.; Ci, R.-N.; Wang, X.-Z.; Wang, Y.; Wang, J.-H.; Chen, B.; Tung, C.-H.; Wu, L.-Z. Quantum dots enable direct alkylation and arylation of allylic C(sp^3)−H bonds with hydrogen evolution by solar energy. *Chem* **2021**, *7* (5), 1244−1257.

(35) Jiang, Y.; Wang, C.; Rogers, C. R.; Kodaimati, M. S.; Weiss, E. A. Regio-and diastereoselective intermolecular [2+ 2] cycloadditions photocatalysed by quantum dots. *Nat. Chem.* **2019**, *11* (11), 1034−1040.

(36) Jiang, Y.; López-Arteaga, R.; Weiss, E. A. Quantum dots photocatalyze intermolecular [2+ 2] cycloadditions of aromatic alkenes adsorbed to their surfaces via van der Waals interactions. *J. Am. Chem. Soc.* **2022**, *144* (9), 3782−3786.

(37) Luo, Y. R. *Handbook of Bond Dissociation Energies in Organic Compounds*; CRC Press, 2002.

(38) Cao, W.; Yakimov, A.; Qian, X.; Li, J.; Peng, X.; Kong, X.; Copéret, C. Surface Sites and Ligation in Amine-capped CdSe Nanocrystals. *Angew. Chem., Int. Ed.* **2023**, *62* (50), No. e202312713.

(39) Huang, C.; Ci, R.-N.; Qiao, J.; Wang, X.-Z.; Feng, K.; Chen, B.; Tung, C.-H.; Wu, L.-Z. Direct Allylic C(sp^3)−H and Vinylic C(sp^2)−H Thiolation with Hydrogen Evolution by Quantum Dots and Visible Light. *Angew. Chem., Int. Ed.* **2021**, *60* (21), 11779−11783.

(40) Dobereiner, G. E.; Crabtree, R. H. Dehydrogenation as a Substrate-Activating Strategy in Homogeneous Transition-Metal Catalysis. *Chem. Rev.* **2010**, *110* (2), 681−703.

(41) Neubert, L.; Michalik, D.; Bähn, S.; Imm, S.; Neumann, H.; Atzrodt, J.; Derdau, V.; Holla, W.; Beller, M. Ruthenium-Catalyzed Selective α,β-Deuteration of Bioactive Amines. *J. Am. Chem. Soc.* **2012**, *134* (29), 12239−12244.

(42) Chatterjee, B.; Krishnakumar, V.; Gunanathan, C. Selective α-Deuteration of Amines and Amino Acids Using D$_2$O. *Org. Lett.* **2016**, *18* (22), 5892−5895.

(43) Takahashi, M.; Oshima, K.; Matsubara, S. Ruthenium Catalyzed Deuterium Labelling of α-Carbon in Primary Alcohol and Primary/Secondary Amine in D$_2$O. *Chem. Lett.* **2005**, *34* (2), 192−193.

(44) Loh, N. D.; Sen, S.; Bosman, M.; Tan, S. F.; Zhong, J.; Nijhuis, C. A.; Král, P.; Matsudaira, P.; Mirsaidov, U. Multistep nucleation of nanocrystals in aqueous solution. *Nat. Chem.* **2017**, *9* (1), 77−82.

(45) Hesk, D.; Borges, S.; Hendershot, S.; Koharski, D.; McNamara, P.; Ren, S.; Saluja, S.; Truong, V.; Voronin, K. Synthesis of (3) H, (2) H4 and (14) C-SCH 417690 (Vicriviroc). *J. Labelled Compd. Radiopharm.* **2016**, *59* (5), 190−196.

(46) Wu, K. J.; Klepacki, D.; Mankin, A. S.; Myers, A. G. A method for tritiation of iboxamycin permits measurement of its ribosomal binding. *Bioorg. Med. Chem. Lett.* **2023**, *91*, 129364.

(47) Hesk, D.; Borges, S.; Dumpit, R.; Hendershot, S.; Koharski, D.; McNamara, P.; Ren, S.; Saluja, S.; Truong, V.; Voronin, K. Synthesis of 3, 2 and 14 3814 (preladenant). *J. Label. Compd. Radiopharm.* **2017**, *60* (4), 194−199.

(48) Cukier, R. I. A Theory that Connects Proton-Coupled Electron-Transfer and Hydrogen-Atom Transfer Reactions. *J. Phys. Chem. B* **2002**, *106* (7), 1746−1757.

(49) Chen, L.; Wang, Q.; Hu, B.; Lafon, O.; Trébosc, J.; Deng, F.; Amoureux, J.-P. Measurement of hetero-nuclear distances using a symmetry-based pulse sequence in solid-state NMR. *Phys. Chem. Chem. Phys.* **2010**, *12* (32), 9395−9405.

(50) Atterberry, B. A.; Carnahan, S. L.; Chen, Y.; Venkatesh, A.; Rossini, A. J. Double echo symmetry-based REDOR and RESPDOR pulse sequences for proton detected measurements of heteronuclear dipolar coupling constants. *J. Magn. Reson.* **2022**, *336*, 107147.

(51) Cunningham, J.; Perras, F. A. INTERFACES. A program for determining the 3D structures of surfaces sites using NMR data. *J. Magn. Reson. Open* **2022**, *12–13*, 100066.

(52) Nishiyama, Y.; Agarwal, V.; Zhang, R. Efficient symmetry-based γ-encoded DQ recoupling sequences for suppression of t1-noise in solid-state NMR spectroscopy at fast MAS. *Solid State Nucl. Magn. Reson.* **2021**, *114*, 101734.

(53) Feike, M.; Demco, D. E.; Graf, R.; Gottwald, J.; Hafner, S.; Spiess, H. W. Broadband Multiple-Quantum NMR Spectroscopy. *J. Magn. Reson., Ser. A* **1996**, *122* (2), 214−221.